d-wave Quasiparticles in the Tilted Vortex Lattice

Michael A. Hermele[1] and Luca Marinelli[2]
[1] *Department of Physics, University of California, Santa Barbara, CA 93106*
[2] *Department of Physics, Harvard University, Cambridge, MA 02138*
(February 1, 2008)

We investigate the quasiparticle spectrum of a d-wave superconductor in the mixed state, focussing on the effects of varying the in-plane angular alignment (or tilting) of the vortex and crystal lattices. Our approach starts with a linearized Bogoliubov-de Gennes equation cast into a simple form by the Franz-Tešanović singular gauge transformation. The zero magnetic field spectrum is characterized by the anisotropy α_D near the four Fermi-surface nodes; at large α_D the model simplifies into a one-dimensional form that provides asymptotic results. Numerical and analytical results are presented and compared with previous studies. We find that tilting can be understood in terms of the one-dimensional model at large α_D. We see a striking dependence on the choice of singular gauge, consistent with earlier results, but do not attempt to resolve the issue of which gauge best describes the microscopic physics.

The low-energy quasiparticle spectrum of a d-wave superconductor in the mixed state has been the focus of recent investigations. As the cuprate materials are believed to have an energy gap with predominately $d_{x^2-y^2}$ symmetry[1,2], such work may prove important for understanding certain probes of low-temperature thermodynamics and transport in a magnetic field. The recent studies have generally restricted their attention to one or two fixed vortex lattice geometries, with or without small distortions to break the Bravais lattice symmetry. However, scanning tunneling microscopy experiments[3] on $YBa_2Cu_3O_{7-\delta}$ (YBCO) in a magnetic field of 6 Tesla at 4.2 Kelvin show an oblique lattice with an angle between primitive vectors of about 77°. This suggests that it may be important to consider a range of vortex lattice geometries if a connection between experiment and the calculated spectra is eventually to be made. In this paper we investigate the low-energy spectrum as the in-plane angular alignment, or tilting, of a square vortex lattice and the underlying crystal is varied (Fig. 1).

In zero magnetic field there are four gapless points on the Fermi surface of a single Cu-oxide plane, and the spectrum linearized in momentum about each of these points takes the form of an anisotropic Dirac cone. Using (x', y') to denote crystal lattice coordinates, throughout this paper we specialize to a $d_{x'y'}$ order parameter and the node at $(0, k_F)$, about which the linearized spectrum is:

$$E(\boldsymbol{k}) = \pm\sqrt{v_F^2 k_{y'}^2 + v_\Delta^2 k_{x'}^2}. \tag{1}$$

Here $v_\Delta = \Delta_0/p_F$, where Δ_0 is the maximum magnitude of the superconducting gap on the Fermi surface, and $\hbar = 1$. The anisotropy of the spectrum is characterized by the ratio $\alpha_D = v_F/v_\Delta$. Experimentally α_D is known to be about 14 for YBCO and 20 for $Bi_2Sr_2CaCu_2O_8$[4]. We study the mixed state spectrum within the framework of the Bogoliubov-de Gennes (BdG) equation[5], generalized to incorporate a d-wave order parameter and linearized in momentum operators about the gap nodes[6–9]. The Franz-Tešanović (FT) singular gauge transformation can then be used to simplify the problem by casting it in the form of an anisotropic two-dimensional (2d) massless Dirac equation with a periodic vector and scalar potential[10]. We will be particularly interested in the spectrum at large values of α_D, where a one-dimensional (1d) model provides asymptotic analytical results[11–13] that can be compared with the full 2d model.

We extend the 2D model of Franz and Tešanović[10] to treat tilting at arbitrary angles. Further details of this model can be found in the studies by Marinelli, Halperin and Simon[14] and Vafek *et. al.*[9]; here we only summarize the main features. The magnetic field satisfies $H_{c1} \ll H \ll H_{c2}$, implying $\xi \ll d \ll \lambda$, where ξ is the Ginzburg-Landau (GL) coherence length, d is on the order of the nearest-neighbor vortex separation and λ is the magnetic penetration depth. We remove the length scales λ and ξ from the problem by taking the magnetic field and the magnitude of the order parameter to be spatially uniform, determining the order parameter phase by a linear GL equation. We do not feed the resulting quasiparticle spectrum back into the BdG equation to find a self-consistent solution, which is a good approximation at low temperatures.

The heart of the FT model is a singular gauge transformation that requires the decomposition of the vortex lattice into A and B sublattices, so that each unit cell contains equal numbers of A and B vortices. The spectrum should be independent of the singular gauge used, but several studies indicate this is not the case. This was first pointed out by Vafek *et. al.*[9] and discussed further in several subsequent works[13,15,16]. We believe this issue may be resolved by implementing appropriate boundary conditions (b.c.) at the vortex cores, where the FT gauge transformation is not valid due to the sharp spatial variation of the order parameter magnitude.

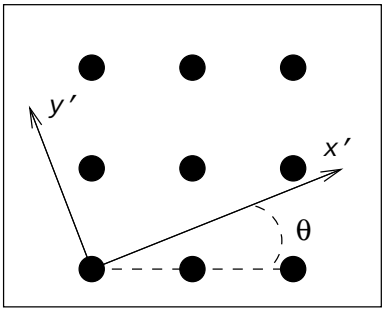

FIG. 1. Schematic view of the intersection of the flux line (vortex) lattice with a single Cu-oxide plane. The magnetic field is perpendicular to the plane, which has an (approximately) square crystal lattice with its orientation described by the x' and y' axes. The crystal axes are tilted by an angle θ from the square lattice of vortex cores, which are represented by the solid circles. Previous work has generally restricted attention to $\theta = 0^\circ$ or 45°.

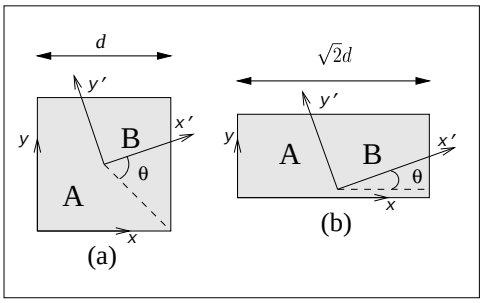

FIG. 2. The magnetic unit cells for two choices of singular gauge. The square $ABAB$ unit cell (a) has side d and is rotated from the underlying vortex lattice by 45°. The rectangular $AABB$ unit cell (b) has long side $\sqrt{2}d$ and is aligned with the vortex lattice. In both cases the distance between nearest-neighbor vortices is $d/\sqrt{2}$, and the tilting of the (x', y') crystal coordinates is measured from the vortex lattice as shown. The (x, y) coordinate system is aligned with the magnetic unit cell.

An analysis of the physics inside the cores will likely be necessary to fix the b.c. appropriately.

We do not attempt to address this issue here, but rather study the unregularized theory in two different singular gauges, each corresponding to a different choice of sublattices. One will be called $ABAB$ (Fig. 2a), the other $AABB$ (Fig. 2b). We work in units where d, the side of the $ABAB$ unit cell, is unity. This results in the following linearized Hamiltonian before singular gauge transformation:

$$\mathcal{H}_{\rm BdG} = \begin{pmatrix} v_F(p_{y'} - \frac{e}{c}A_{y'}) & \frac{1}{p_F}\{p_{x'}, \Delta(\boldsymbol{r})\} \\ \frac{1}{p_F}\{p_{x'}, \Delta^*(\boldsymbol{r})\} & -v_F(p_{y'} + \frac{e}{c}A_{y'}) \end{pmatrix}. \quad (2)$$

Here $\Delta(\boldsymbol{r})$ gives the spatial variation of the GL order parameter in the magnetic unit cell unit cell, which is aligned with the x and y axes (Fig. 2). Upon making the FT transformation and exploiting Bloch's theorem to write an effective Hamiltonian at every point (k_x, k_y) of the first vortex lattice Brillouin zone, one obtains

$$\begin{aligned} \mathcal{H}^{eff}(\boldsymbol{k}) =& (p_{y'} + k_{y'} + \mathcal{A}_{y'})\sigma_3 \quad (3) \\ &+ \frac{1}{\alpha_D}(p_{x'} + k_{x'} + \mathcal{A}_{x'})\sigma_1 + \Phi, \end{aligned}$$

where we have set $v_F = 1$. $\boldsymbol{\mathcal{A}} = \frac{m}{2}(\boldsymbol{v}_s^A - \boldsymbol{v}_s^B)$ is the effective vector potential and $\Phi = \frac{m}{2}(v_{sy'}^A + v_{sy'}^B)$ the effective scalar potential. $\boldsymbol{v}_s^{A,B}$ is the superfluid velocity associated with the A, B sublattice.

Many of the results of Ref. 14 still hold for this tilted Hamiltonian. In particular, the zero energy degenerate doublet at the Brillouin zone center (Γ point) is preserved to all orders in perturbation theory, since this result requires only particle-hole symmetry and a Bravais vortex lattice[14]. Also, except for special tilt angles and anisotropies, we expect no zeroes at other points in the zone. This is because tilting spoils the high symmetry status of the $k_y = 0$ axis where it was found there could be zeroes[14]. However, invariance under $\boldsymbol{k} \to -\boldsymbol{k}$ is preserved. We can therefore restrict our attention to the Γ point to understand the very-low-energy band structure and density of states (DOS).

As pointed out by Vishwanath[15], the splitting in the band structure near any degenerate doublet can be shown by first-order perturbation theory to be an anisotropic Dirac cone to linear order in the k-space displacement. This actually gives the exact result for the slope of the lowest-energy bands as the Γ point is approached from a particular direction. Writing $\boldsymbol{k} = k(\cos\phi, \sin\phi)$, we have

$$\mathcal{H}^{eff}(\boldsymbol{k}) = \mathcal{H}^{eff}(\boldsymbol{0}) + k[\sin(\phi - \theta)\sigma_3 + \frac{1}{\alpha_D}\cos(\phi - \theta)\sigma_3]. \quad (4)$$

An elementary degenerate perturbation theory calculation gives the perturbed energies near the Γ point:

$$\epsilon_\pm = \pm k\sqrt{t_1 \sin^2(\phi - \theta) + t_2 \cos^2(\phi - \theta) + t_3 \sin(2(\phi - \theta))} + \mathcal{O}(k^2), \quad (5)$$

where the coefficients can be expressed in terms of matrix elements of σ_1 and σ_3 between the states of the degenerate doublet. Except for the orientation of the new anisotropy axes, the anisotropic Dirac cone described by Eq. 5 is completely characterized by the maximum and minimum values of ϵ_+/k, which we denote by v_+ and v_-, respectively. We will study these velocities as a function of α_D and θ.

In order to apply the 1d model to obtain information at large α_D, we must specialize to rational tilt an-

gles $\theta = \arctan(p/q)$ for integer p and q. Details of this model are presented in the papers of Knapp, Kallin and Berlinsky[12], and Marinelli and Halperin[13]. The essential idea is that as $\alpha_D \to \infty$ the quasiparticles see vortices that are effectively smeared out in the "hard" v_F-direction, so that all gauge-invariant quantities become functions only of the coordinate in the v_Δ-direction. Choosing coordinates x and y for the soft and hard directions, respectively, the 1d Hamiltonian for crystal momentum $\boldsymbol{k}$ is:

$$\mathcal{H}_{1d}(\boldsymbol{k}) = \begin{pmatrix} k_y + U^A(x) & \frac{1}{\alpha_D}(p_x + k_x) \\ \frac{1}{\alpha_D}(p_x + k_x) & -k_y + U^B(x) \end{pmatrix}. \qquad (6)$$

Here $U^{A,B}$ is the potential encapsulating the residual effects of the A, B vortices. For the gauges considered we can always choose a unit cell with only two columns of smeared-out vortices, provided θ is rational. This is true because the perpendicular distance from one column of A/B vortices to the nearest A/B column is always the same.

There are essentially two distinct possibilities when we go to the 1d model, which depend on the gauge choice and on θ. These are illustrated in Figure 3. Configurations with distinct columns of A and B vortices (Fig. 3a) were shown[13] to give rise to band structure features exponentially small in α_D. In particular, for the $ABAB$ gauge with $\theta = 45°$, it was found that $v_- \sim \exp(-\alpha_D \pi^2/16)$. This can easily be generalized when the distance between two adjacent columns (of different types) is always the same, by scaling the 1d unit cell by a factor of $1/d_v$ in the x-direction and d_v in the y-direction, where d_v is the distance between adjacent vortices in the same column. Following the calculation of Ref. 13 one finds $v_- \sim \exp(-\alpha_D \pi^2/16 d_v^2)$.

When the A and B columns overlap (Fig. 3b) the asymptotic behavior is very different. It has been argued and verified numerically that there are in this case *no* exponentially small features in the band structure[13]. We can go further to calculate the exact 1D band structure on the $k_y = 0$ line, and hence also v_-. Since $U^A = U^B = U(x)$ in this case, we have

$$\mathcal{H}_{1d}(k_x, 0) = U(x) + \frac{1}{\alpha_D}(p_x + k_x)\sigma_1. \qquad (7)$$

The matrix structure of this Hamiltonian is trivial, and it separates into two uncoupled components. The resulting differential equations are:

$$U(x)\psi \pm \frac{1}{\alpha_D}(-i\frac{d}{dx} + k_x)\psi = E_\pm \psi. \qquad (8)$$

Upon integration one finds

$$\psi(x) = \psi_0 e^{\pm i\alpha_D \int^x (E_\pm - U(x) \mp k_x/\alpha_D)}. \qquad (9)$$

ψ is a Bloch function, so we must impose periodic boundary conditions, thus obtaining a quantization condition

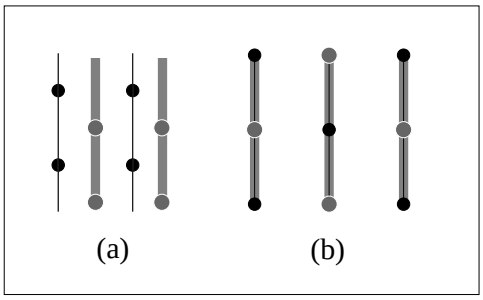

FIG. 3. Diagram of the two qualitatively different configurations of the 1d model. Dark circles/lines represent one type of vortex/column of vortices. The shaded circles and lines represent the other. In (a) the A and B vortices form distinct columns, while in (b) all columns contain equal numbers of A and B vortices.

for the energies:

$$\int_{-1/2d_v}^{1/2d_v} dx(E_\pm - U(x) \mp \frac{k_x}{\alpha_D}) = \frac{2\pi n}{\alpha_D}. \qquad (10)$$

For those solutions with $|E|$ greater than the maximum of $U(x)$, this is exactly the Bohr-Sommerfeld quantization condition used in Ref. 13 to obtain the spectrum in a WKB approximation[13], only here it is exact. At the Γ point ($k_x = 0$), there are doubly degenerate solutions $E_\pm = E_n^\Gamma$. The degeneracy is split for finite k_x and $E_\pm = E_n^\Gamma \pm k_x/\alpha_D$ (see Figs. 10 and 11 in Ref. 13). The lowest bands are simply $E_\pm = \pm k_x/\alpha_D$, implying $v_- = 1/\alpha_D$ in striking contrast to the case of separated columns. Still more striking is the fact that we can switch between exponential (separated columns) and algebraic (overlapping columns) decrease of v_- simply by choosing a different singular gauge. For example, if the gauge choice did not matter the $AABB$ lattice with $\theta = 45°$ would be the same as $ABAB$ and $\theta = 0°$. But the spectra are *not* the same, since the former case has overlapping columns in the 1D model and the latter does not. These conclusions are in excellent agreement with the numerical results[13].

We have numerically calculated $v_\pm$ as a function of α_D and θ in the 2d model with a reciprocal space cutoff. Working in momentum space allows tilting to be handled very simply, and avoids the complications associated with discretizing a Dirac equation on a real space lattice[14,17]. The major disadvantage is that the matrices to be diagonalized are not sparse. For the square unit cell of the $ABAB$ gauge we typically used a cutoff of $\Lambda = 10$, where $|Q_x|, |Q_y| \leq \Lambda$ and Q_i are the coefficients of the reciprocal lattice primitive vectors. For the $AABB$ gauge the unit cell is non-square, so we took $2|Q_x|, |Q_y| \leq \Lambda$, typically with $\Lambda = 8$. It was not feasible to push Λ much greater than 20. Also, for any fixed Λ, we expect the numerical calculations to become less reliable as α_D is increased, since raising the anisotropy introduces more and more low-energy states that do not fall within the

cutoff and are improperly thrown out. Although the accessible range of Λ and α_D is not sufficient to provide detailed information on the true asymptotic behavior as $\alpha_D \to \infty$ or the convergence of the numerics, we believe it should be sufficient to extract certain important qualitative features.

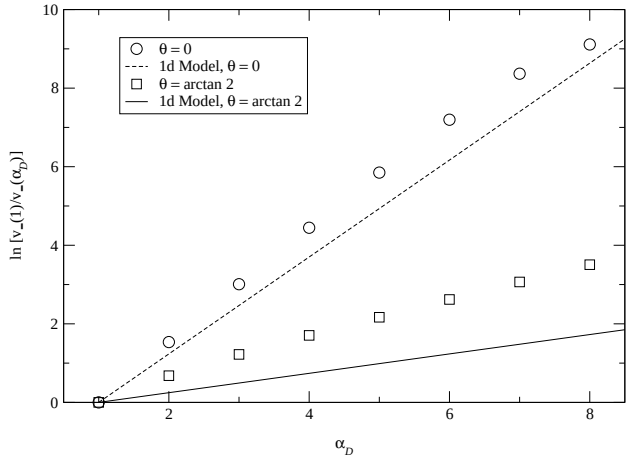

FIG. 4. Plot of $\ln(v_-(1)/v_-(\alpha_D))$ versus the anisotropy α_D, comparing data from the 2d numerics with the 1d model. The results shown are in the $AABB$ gauge, with tilt angles giving distinct columns in the 1d model. The hollow shapes are numerical results for $\theta = 0$ and $\theta = \arctan 2$. The lines are the asymptotic results from the 1d model and have slope $\pi^2/(16 d_v^2)$.

Our results for $v_-(\alpha_D)$ at fixed θ show good qualitative agreement with the predictions of the 1d model. For tilt angles and gauges with distinct A and B columns we see roughly exponential decrease of v_- similar to that calculated analytically (Fig. 4). We believe we do not see quantitative agreement because we cannot access the asymptotic regime numerically. When there are overlapping columns we see similar agreement with the analytical results; v_- is roughly proportional to $1/\alpha_D$ with the constant of proportionality closer to unity when the columns are farther apart (Fig. 5). This is consistent with our understanding of the 1d model; at greater column separation d_v is smaller, and the quasiparticle wavefunctions do not have to be smeared out as much for them to be completely delocalized in the y-direction. Numerical calculations of v_+ show only small variations, typically by at most a factor of order unity as α_D ranges from 1 to 8. Therefore the renormalized anisotropy v_+/v_- behaves similarly to $1/v_-$ as a function of α_D.

We have seen that, for large α_D, tilting of the vortex and crystal lattices in the Franz-Tešanović framework can be understood in terms of a one-dimensional model. For tilt angles and singular gauges with distinct columns of A and B vortices, v_- is exponentially small in α_D, while when the columns overlap it decreases algebraically. In both these cases v_+ does not vary significantly with α_D. These results depend dramatically on the choice of singular gauge, and provide a further indication that the FT transformation must somehow be regularized if it is to provide a consistent account of the physics. While proposals for the kind of regularization necessary have been discussed in the literature[13,15,16], a detailed resolution of these issues remains an important problem for future work.

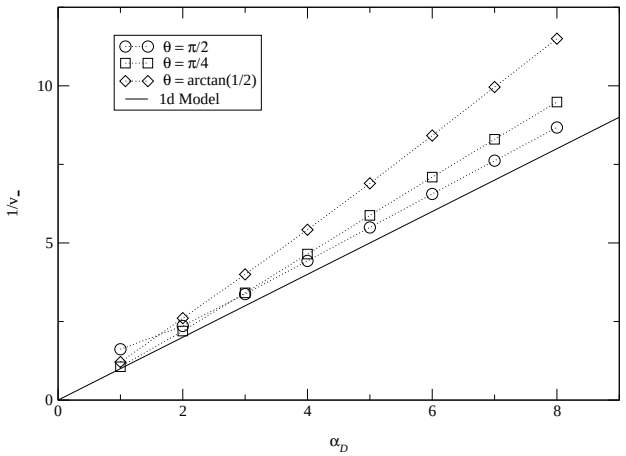

FIG. 5. Plot of $1/v_-$ versus α_D comparing 2d numerical data in the $AABB$ gauge with the 1d model. The tilt angles are chosen to give overlapping columns of vortices in the 1d model. The shapes connected by dotted lines are 2d numerical data for different tilt angles, and the solid line is simply a plot of $1/v_- = \alpha_D$, the exact 1d result.

The authors would like to thank B.I. Halperin for very useful discussions and a careful reading of the manuscript. MH was supported by the Harvard MRSEC NSF/DMR-9809363 through the REU program, by the Department of Defense with an NDSEG fellowship, and by Regents Special and Broida Fellowships from the University of California, Santa Barbara. LM was supported in part by the NSF grant DMR-99-81283.

[1] D. J. Van Harlingen, Rev. Mod. Phys. **67**, 515 (1995).
[2] C. C. Tsuei and J. R. Kirtley, Rev. Mod. Phys. **72**, 969 (2000).
[3] I. Maggio-Aprile, Ch. Renner, A. Erb, E. Walker and Ø. Fischer, Phys. Rev. Lett. **75**, 2754 (1995).
[4] May Chiao *et. al.*, Phys. Rev. B **62**, 3554 (2000).
[5] P. G. de Gennes, *Superconductivity of Metals and Alloys* (Addison-Wesley, Reading, MA, 1989).
[6] S. H. Simon and P. A. Lee, Phys. Rev. Lett. **78**, 1548 (1997).
[7] G. E. Volovik and N. B. Kopnin, Phys. Rev. Lett. **78**, 5028

(1997).
[8] S. H. Simon and P. A. Lee, Phys. Rev. Lett. **78**, 5029 (1997)
[9] O. Vafek, A. Melikyan, M. Franz and Z. Tešanović, Phys. Rev. B **63**, 134509 (2001).
[10] M. Franz and Z. Tešanović, Phys. Rev. Lett. **84**, 554 (2000).
[11] A. S. Mel'nikov, J. Phys.: Condensed Matter **11** 4219 (1999).
[12] D. Knapp, C. Kallin and A. J. Berlinsky, Phys. Rev. B **64**, 014502 (2001).
[13] Luca Marinelli and B. I. Halperin, Phys. Rev. B **65**, 014516 (2002).
[14] Luca Marinelli, B. I. Halperin and S. H. Simon, Phys. Rev. B **62**, 3488 (2000).
[15] Ashvin Vishwanath, Phys. Rev. Lett. **87**, 217004 (2001).
[16] O. Vafek, A Melikyan and Z. Tešanović, Phys. Rev. B **64**, 224508 (2001).
[17] J. B. Kogut, Rev. Mod. Phys. **55**, 775 (1983).